Proc. of the Fourth Intl. Conf. Advances in Civil, Structural and Mechanical Engineering- CSM 2016

ISBN: 978-1-63248-093-4 doi: 10.15224/ 978-1-63248-093-4-18

Hot Corrosion Resistance of $La_2Zr_2O_7$ Coat on Stainless Steel Alloy

S. M. Naga, M. Awaad, H. F. El-Maghraby, A. M. Hassan, Mohamed Elhoriny, Andreas Killinger, Rainer Gadow

Abstract— In the present study, $La_2Zr_2O_7$ was used as a coat for stainless steel alloy. Lanthanum zirconate coat was sprayed using plasma spray technique. The preparation and characterization of $La_2Zr_2O_7$ coat was studied. Hot corrosion of the coat surface was conducted in (1:1) V_2O_5 / Na_2SO_4 molten mixture at 900°C for 50 and 100 h. The results showed that molten mixture of V_2O_5 / Na_2SO_4 attacks $La_2Zr_2O_7$ coat heavily after 100 h. Depending on the nature of molten salt, $La_2Zr_2O_7$ can considered either a strong basic oxide or strong acidic oxide.

***Keywords*— Plasma coating, Lanthanum zirconate, Hot corrosion resistance**

Salma M. Naga/ Professor
Ceramics Dept/National Research Center
Egypt

M. Awaad/ Professor
Ceramic Dept/National Research Center
Egypt

Hesham. F. El-Maghraby/ PhD
Ceramics Dept/National Research Center
Egypt

Ahmed. M. Hassan/ PhD
Faculty of Engineering/Zagazig university
Egypt

Mohamed Elhoriny/ MSc
Graduate School of Excellence Advanced Manufacturing Engineering (GSaME)/ Stuttgart University

Andreas Killinger / Professor
Institute for Manufacturing Technologies of Ceramic Components and Composites (IMTCCC)/ Stuttgart University

Rainer Gadow/ Professor
Institute for Manufacturing Technologies of Ceramic Components and Composites (IMTCCC)/ Stuttgart University

I. Introduction

For decades YSZ was the material of choice for thermal barrier coatings (TBCs), as it possesses low thermal conductivity and relatively high thermal coefficient that reduces the thermal expansion mismatch with the metallic substrate [1,2]. Due to the limited operation temperature for long-term applications of YSZ, researchers sought for new materials. Rare-earth zirconates ($M_2Zr_2O_7$) are investigated as alternatives for YSZ. They have two crystalline forms; ordered pyrochlore structure and disordered fluorite one [3]. The thermal stability and low thermal conductivity pointed pyrochlore zirconate as an interesting material for TBC applications. Pyrochlore $La_2Zr_2O_7$ (PLZ) is a significant candidate for TBC topcoat. Because of its low oxygen content; it has a better bond coat oxidation resistance in comparison to YSZ [4]. PLZ possesses cubic structure that consists of octahedra ZrO_6 at the corners; forming the backbone of the structure; and La^{3+} ions filling the holes formed by ZrO6 octahedra [5].

$La_2Zr_2O_7$ is synthesized by various methods like, conventional solid-state reaction, co-precipitation, sol-gel, hydrothermal and molten salts methods [6-8]'. Ramachandran et al [9] used transferred arc plasma (TAP) melting to produce lanthanum zirconate. They observed a variation in the LZ stoichiometry after TAP melting. They claimed that the variation is due to the evaporation of La_2O_3 from the mixture. Cao et al [10] suggested that doping of LZ with some elements, increasing the content of La_2O_3 in the LZ starting material and applying gradient coating with YSZ, could improve the thermal cycling life of LZ coating. Increasing the thermal expansion coefficient of LZ is an important issue, as its thermal expansion is relatively low (~ 9 X 10-6/°k). Low thermal expansion leads to thermal expansion mismatch and high thermal stresses [2].

II. Materials and Methods

A. *Materials*

For the preparation of lanthanum zirconate ($La_2Zr_2O_7$), chemically pure reagents of La_2O_3, 99.99%-La (Strem Chemicals, Newburyport, MA, USA) and zirconium n-(IV) butoxide (Strem Chemicals, Newburyport, MA, USA) were used.

Proc. of the Fourth Intl. Conf. Advances in Civil, Structural and Mechanical Engineering- CSM 2016

ISBN: 978-1-63248-093-4 doi: 10.15224/ 978-1-63248-093-4-18

B. *Preparation of Lanthanum Zirconate*

Predetermined amounts of zirconium tetra-n-butoxide and lanthanum oxide were carefully weighed. Zirconium alkoxide amount was rapidly dissolved in absolute ethanol with stirring till complete mixing. An amount of nitric acid just sufficient to break the metal-alkoxide bonds (3-5 ml) was added to the mixture. The zirconium alkoxide and nitric acid mixture was then hydrolyzed with the addition of 1:1 water/ethanol mixture and vigorous stirring for 2 h at 80°C. The hydrolyzed zirconium alkoxide was peptized with the addition of 3 ml nitric acid, which led to a transparent sol, and then was left to cool. Meanwhile, lanthanum oxide was dissolved in hot diluted nitric acid. The formed lanthanum nitrate solution was evaporated to almost dryness to get rid of the excess nitric acid, and was mixed with the previously hydrolyzed zirconium alkoxide. The transparent sol mixture was left at room temperature till gel formation. The gel was dried at 110 °C till complete dryness and then calcined in an electric oven (Nabertherm, Germany) for 2 h at 700 °C in static air to get rid of all organic and nitrate species. The calcined gel was then heated up to 900, 1000 and 1100°C for 2 h to follow up the progress of $La_2Zr_2O_7$ phase formation. The powder was ground in an automatic agate mortar and pestle to eliminate the agglomerations.

C. *Plasma Coating*

Atmospheric plasma spraying (APS) technique was used to deposit lanthanum zirconate coating on stainless steel 1.4301 from Scholz-Edelstahl (Germany). A F6 torch from GTV (Germany) was used for the deposition and was guided through a six axes robot of type RX130B from Stäubli Tec-System GmbH (Germany).

Before spraying, the substrates' surfaces were provided with roughening asperities by means of undergoing grit blasting using F60 corundum particles, which were propelled at a pressure of 6 bars. This proved useful in increasing the mechanical interlocking, and therefore, adhesion between the deposited coating splats and the substrate. The deposition was done by applying a meander path; Fig.1; using the spraying parameters mentioned in Table 1.

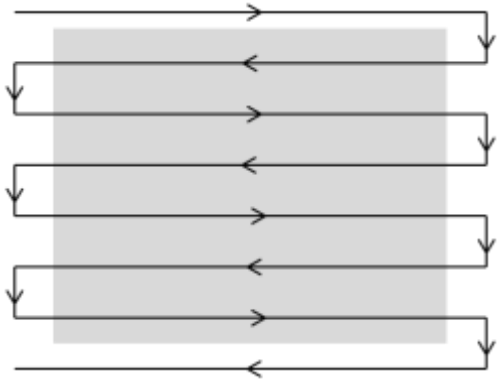

Figure. 1. meander path deposition.

TABLE. 1. SPRAYING PARAMETERES.

Parameter	Value
Stand-off distance	130 [mm]
Robot speed	600 [mm/s]
Offset	3 [mm]
Power feed rate	50 [g/min]
Carrier gas flow rate	Ar at 7 [l/min]
Plasma gases	Ar/ H_2 at 40/8 [l/min]
Forced air cooling	Front side of substrate

D. *Hot Corrosion Test*

The hot corrosion test was carried out on the coated sample of dimensions 10 mm X 10 mm X 3 mm. (1:1) V2O5/Na2SO4 mixture was applied uniformly over the coatings surface to coverage of 10 mg/cm2. The sample was heated at 900°C in air for different periods of 50, and 100 h. After cooling, the sample was collected for surface study by using both thin layer XRD and microstructural investigations.

E. *Characterization*

XRD of powdered samples was applied to identify crystalline phases with goniometric range 20–80º and scan speed of 1º/min (Philips 1730 diffractometer with a Ni-filtered and monochromated Cu Kα radiation). Care was taken to maintain the current at 40 kV and 40 mA during the experiment. TEM (Jeol 1230, Japan) was conducted on the prepared powders to examine their grain size. The morphological and microstructural characteristics were evaluated by the scanning electron microscope (SEM-Jeol JSM-T20).

III. Results

F. *Starting Materials Characterization*

TEM micrograph of the lanthanum zirconate gel calcined at 900 ºC for 1 h showed that its grain size is in the range of 38-66 nm, Fig. 2.

The X-ray diffraction analysis of the gel calcined at 900, 1000 and 1100 ˚C is shown in Fig. 3. It is clear from the figure that increasing the calcination temperature increases the phase crystallinity. It also, shows that complete crystallization into lanthanum zirconate (pyrochlore) starts to take place at 900 ºC. No other crystalline phases were detected under the conditions of the experiment.

Proc. of the Fourth Intl. Conf. Advances in Civil, Structural and Mechanical Engineering- CSM 2016

ISBN: 978-1-63248-093-4 doi: 10.15224/ 978-1-63248-093-4-18

Phase composition (XRD) of the coat showed that it composed totally of lanthanum zirconate, Fig.4. Its microstructure general view shows that the LZ coat thickness is ~ 50.68 µm, Fig. 5. The detailed microstructure of the coat layer is shown in Fig.6.a. It shows many cracks within the coat, nanoscale LZ grains and relatively large pores. The nanocrystalline structure of LZ was preserved by the short dwell time that LZ powder experienced during plasma spraying. The rapid cooling of the powders is also led to the presence of the nanoscale grains of LZ [11]. Berndt et al and Zhu et al also mentioned this observation in their studies [12,13]. The presence of Fe, Cr and Ni oxides in the EDS spectrum of the interface, Fig. 6.b, indicates the reaction between the substrate and the coat layer. Shane and Mecartne [14] claimed that the interfacial reactions strengthening the interface between the substrate and the ceramic coat. Higher magnification of the LZ coat layer is shown in Fig.7. It shows a lamellar, porous structure characteristic for plasma spray coating [15]. The interlamellar pores are resulting from the rapid solidification of the lamella, the cracks developed from the thermal stresses and tensile quenching relaxation stresses and the fine voids formed around the non-melted particles or by the incomplete intersplat contact [16].We believe that the amount of melted particles to fill surface irregularities is not enough, which leads to the formation of pores between splats. Also, the presence of non-flattens non-molten/partially melted grains results in a very small area of intimate contact with other particles and the creation of large pores between the grains [17].

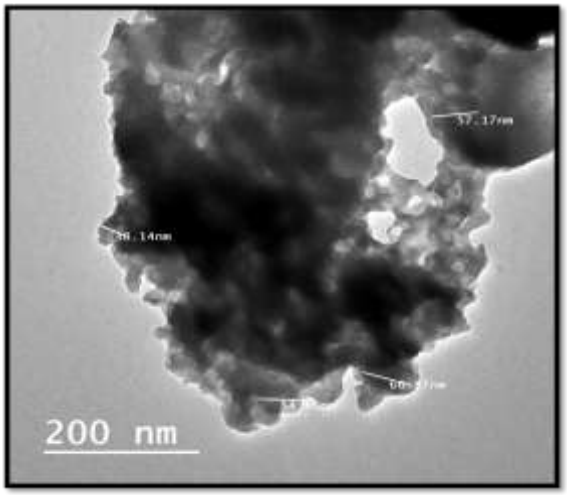

Figure. 2. TEM micrograph showing that lanthanum zirconate particle size.

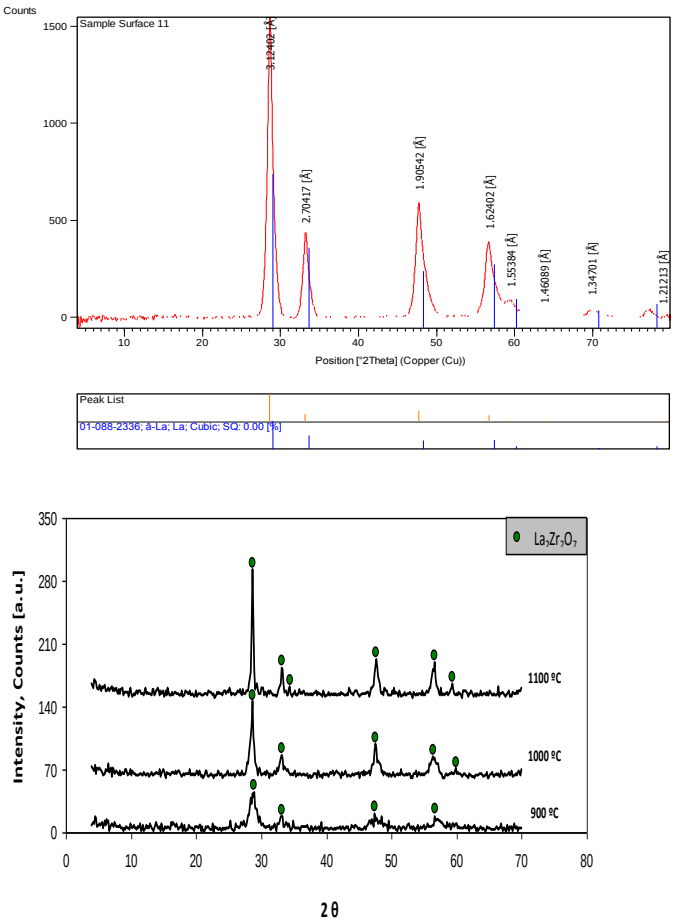

Figure. 3. XRD pattern of LZ powder calcined at different firing temperatures.

Figure. 4. XRD of surface layer coat.

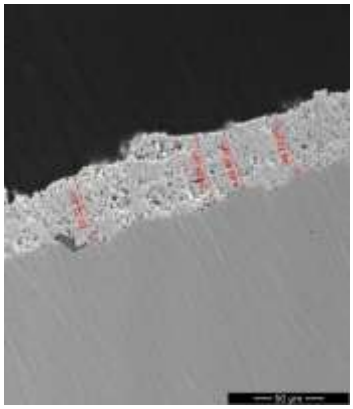

Figure. 5. General view and coat thickness of the sample.

It is to be noticed that when $La_2Zr_2O_7$ coat hot treated with Na_2SO_4/V_2O_5 mixture it shows heavily attacked surface. Figures 8.a and 9a show many corrosive pores, which are due to the deterioration of the coat by vanadium and sulfate salts. There are two different corrosion products are observed in the samples hot treated for 50 h; namely block –shaped and particle-shaped. EDS analysis identified the hot corroded products to be $LaVO_4$ for the block –shaped and $La_2Zr_2O_7$ for particle- shaped, Fig. 8.b and c.

Proc. of the Fourth Intl. Conf. Advances in Civil, Structural and Mechanical Engineering- CSM 2016

ISBN: 978-1-63248-093-4 doi: 10.15224/ 978-1-63248-093-4-18

Depending on the molten salts $La_2Zr_2O_7$ can consider either a strong basic oxide former or strong acidic oxide. From the phase diagram of Na_2SO_4 - V_2O_5 binary diagram system [18] and based on the reaction conditions used in the present study Na_2SO_4 and V_2O_5 will react according to the following equation:

$$Na_2SO_{4\,(l)} + V_2O_{5\,(l)} \longrightarrow 2\,NaVO_{3\,(l)} + SO_{4\,(g)} \quad (1)$$

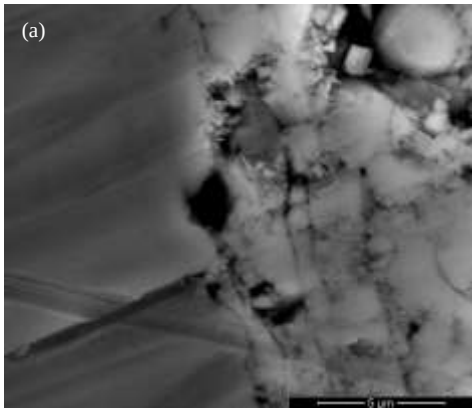

(b)

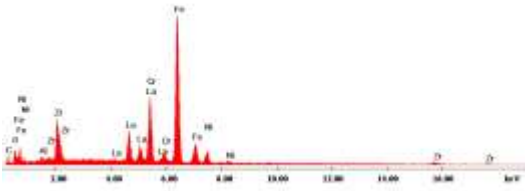

Figure. 6. SEM micrograph of the sample layer: (a) nanoscale LZ grains and cracks within LZ coat (b) The interface between LZ and the metallic substrate.

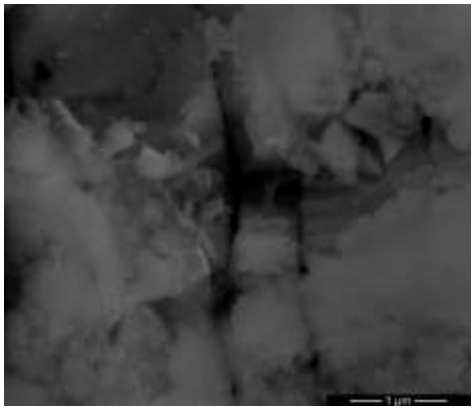

Figure. 7. Lamellar, porous structure of LZ coat.

According to Rapp [19] the presence of $NaVO_3$ will enhance the acidic solubility and $La_2Zr_2O_7$ will react with $NaVO_3$ according to the equation:

$$2\,NaVO_{3\,(l)} + La_2Zr_2O_{7\,(s)} \longrightarrow 2\,ZrVO_{7\,(s)} + 2LaVO_{4\,(s)} + Na_2O_{(l)} \quad (2)$$

But $ZrVO_7$ melts incongruently at ~ 747 ºC to form m-ZrO_2 and a mixture of m- ZrO_2 and V_2O_5 [20,21]. Accordingly, the hot corrosion mechanism in this case could be:

$$2NaVO_{3\,(l)} + La_2Zr_2O_{7\,(s)} \longrightarrow 2\,LaVO_{4\,(s)} + 2m\text{-}ZrO_{2\,(s)} + Na_2O_{(l)} \quad (3)$$

Due to the low boiling point of Na_2O; 882.9 ºC; Na_2O will evaporate and Na-containing phases will be undetectable. With increasing the heat treatment time to 100 h, Na_2SO_4 /V_2O_5 mixture aggressively attack the ZrO_2 coat, according to the reaction:

$$ZrO_{2\,(s)} + V_2O_{5(l)} \longrightarrow ZrV_2O_{7\,(s)} \quad (4)$$

The obtained products are well-crystallized rod-like shape $LaVO_4$ and corroded areas containing Cr and Fe oxides; Fig.9a. EDS analysis, Fig.9b, shows the chemical analysis of the examined area.

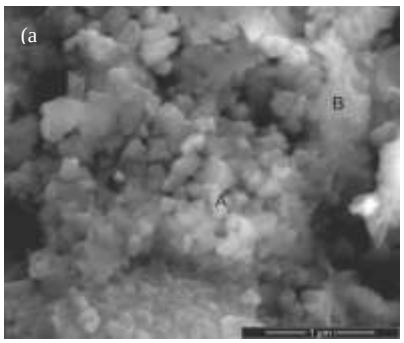

(b

(c

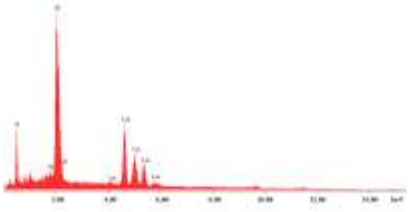

ISBN: 978-1-63248-093-4 doi: 10.15224/ 978-1-63248-093-4-18

Figure. 8. SEM micrograph of the sample: (a) block and particle shaped microstructure of 50h treated sample, (b) EDS spectra of LaVO4 particles, (c) EDS spectra of La2Zr2O7 particle.

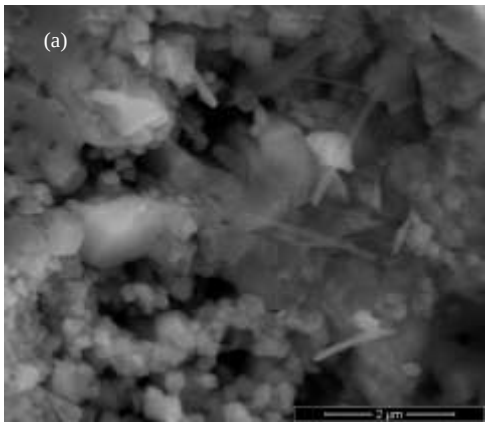

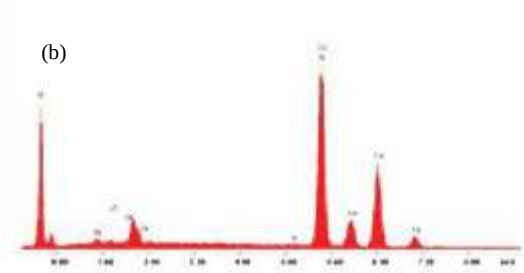

Figure. 9. SEM micrograph of the sample heated for 100h at 900 ˚C, (a) well-crystallized rod-like shape LaVO4 and corroded areas containing Cr and Fe oxides, (b) EDS spectra of the examined sample..

IV. Conclusions

1- Pure nano- size Lanthanum zirconate phase was prepared using the sol- gel technique with particle size of 38- 66 nm.

2- $La_2Zr_2O_7$ coat suffered from severe corrosion when exposed to a molten mixture of Na_2SO_4/V_2O_5 (1:1) for 100 h.

3- Two different corrosion products are observed in the hot treated samples treated with molten salt mixture for 100 h; block –shaped and rod like $LaVO_4$ grains and solid solution of Fe and Ni.

V. References

[1] X. Cao, R. Vassen, and D. Stoever, “Ceramic materials for thermal barrier coatings”, J. Eur. Ceram. Soc., vol. 24, pp. 1-10, 2004.

[2] R. Vassen, M. O. Jarligo, T. Steinke, D. E. Mack and D. Stoever, “Overview on advanced thermal barrier coatings”, Surf. Coat Technol., vol. 205, pp. 938-942, 2010.

[3] D. J. M. Bevan and E. Summerville, “Mixed rare earth oxides”. Handbook on Physics and Chemistry of Rare Earths: Non Metalic CompoundsI. Edited by Gschneider, K.A., Eyring, L.R. Physics Publisher, North-Holland, New York, 1979.

[4] S. Yugeswaran, A. Kobayashi, P. V. Ananthapadmanabhan and L. Lusvarghi, “ Influence of processing variables on the formation of $La_2Zr_2O_7$ in transferred arc plasma torch processing”, Curr. Appl. Phys., 11, 1394-1400, (2011).

[5] M. A. Subramanian, G. Aravamudan and G. V. S. Rao, “Oxide pyrochlore-A review”, Prog. Solid State Chem., vol. 15, pp. 55-143, 1983.

[6] K. K. Rao, T. Banu, M. Vithal, G. Y. S. K. Swamy and K. R. Kumar, “Preparation and characterization of bulk and nano particles of $La_2Zr_2O_7$ by sol-gel method”, Mater. Lett., vol. 54, pp. 205-210, 2002.

[7] J. Nair, R. Nair, E. B. M. Doesburg, J. G. Van omen, J. R. H. Ross and A.G. Burggraaf, “Preparation and characterization of lanthanum zirconate”, J. Mater. Sci., 33, 4517-4523, (1983).

[8] X. Wang, Y. Zhu and W. Zhang, “Preparation of lanthanum zirconate nano-powders by molten salts method”, J. Non-Cryst. Solids., vol. 356, pp. 1049-1051, 2010.

[9] C. S. Ramachandran V. Balasubramanian and P. V. Ananthapadmanabhan, “Synthesis, spheroidization and spray deposition of lanthanum zirconate using thermal plasma process”, Surf. Coat. Technol., vol. 206, pp. 3017-3035, 2012.

[10] X. Q. Cao, R. Vassen, W. Jungen, S. Schwartz, F. Tietz and D. Stoever, “Thermal stability of lanthanum zirconate plasma sprayed coatings”, J. Am. Ceram. Soc., vol. 84, no. 9, pp. 2086-2090, 2001.

[11] X. Wang, Y. Zhu, L. Du and W. Zhang, “The study on porosity and thermophysical properties of nanostructured $La_2Zr_2O_7$ coatings”, Appl. Surf. Sci., vol. 257, pp. 8945-8949, 2011.

[12] C. Berndt and E. J. Larenia, “Thermal spray processing of nanoscale materials”, J. Therm. Spray Technol., vol. 7 , pp. 411-440, 1998.

[13] Y. Zhu, M. Huang, J. Huang and C. Ding, “Vacuum – plasma sprayed nanostructured titanium oxide films”, J. Therm. Spray Technol., vol. 8, pp. 219- 222, 1999.

[14] M. Shane and M. L. Mecartney, “Sol-gel sunthesis of zirconia barrier coatings”, J. Mater. Sci., vol. 25, pp. 1537-1544, 1990.

[15] C. J. Li, Y. He and A. Ohmuri, “Characterization of structure of thermally sprayed coating”, proceeding of the 15th International thermal spray conference, Nice, France, 1998.

[16] G. Shanmugavelayutham and A. Kobayashi, “Mechanical properties and oxidation behavior of plasma sprayed functionally graded zirconia-alumina thermal barrier coatings”, Mater. Chem. Phys., 103, 283-289, (2007).

[17] A. Kulkarni, A. Vaidya, A. Goland, and A. Sampath, “Processing effects on porosity corelations in plasma sprayed yttria-stabilized zirconia coatings”, Mater. Sci. Eng. A, vol. 359, pp. 100-111, 2003.

[18] G. Smith, “Phase diagrams for ceramists”. vol. IV, Columbus, OH, 1981, Fig.5127.

[19] R. A. Rapp, “Hot corrosion of materials: a fluxing mechanism”, Corros. Sci., vol. 44, no. 2, pp. 209-221, 2002.

[20] M. K. Reser, “Phase diagrams for ceramists”. Eds. Columbus, OH, Supplement, American Ceramic Society, 1969, (Fig. 2405).

[21] R. C. Buchanan and G. W. Wolter, “Properties of hot-pressed zirconium pyrovanadate ceramics”, J. Electrochem. Soc., vol. 130, no. 4, pp. 1905-1910, 1983.

Prof. Dr. Salma M. Naga, earned her Ph.D. from Cairo University in 1983. She is currently Professor of Ceramics Chemistry and Technology at the National Research Centre, Cairo, Egypt.